

Role of melatonin as a protective antioxidant in the amelioration of oxidative stress mediated tissue injury: a new vision for futuristic medicine

Debasish Bandyopadhyay

ABSTRACT

Melatonin (N-acetyl-5-methoxy tryptamine) is ubiquitous in almost every creature; diatoms, bacteria, plants, and animals. During the course of organic evolution, melatonin (a pineal secretory product in vertebrates and mammals, including humans) never changed its structure and thus remain conserved as an ancient molecule in nature. Since discovery of the antioxidant properties of melatonin by Dr. Dun-Xian Tan in 1993, its antioxidative efficacy in various situations of oxidative stress in plants, animals and humans has been well established. It is clear that melatonin has evolved much earlier than other antioxidants. Ischaemic heart disease (IHD) and consequential myocardial infarction (MI) is a health problem of global concern and its ubiquitous prevalence is increasing worldwide annually. The involvement of oxidative stress in myocardial ischemia has long been recognized around the globe. Moreover, the prescribed medicines for cardiac tissue well-being sometimes became detrimental for gastric epithelium. Though endogenous gastric melatonin plays a protective role in offering protection to the entire gastric system, stress-mediated challenged melatonin level brings about threats to the gastric system. Mitigation of oxidative stress in the myocardium and gastric system as well, by antioxidants, may play an effective role in protection and the results of our studies carried out through several years have revealed that melatonin offers extensive protection toward the said systems when subjected to stress by physiological as well as synthetic molecules. Further, we have extrapolated our studies to check whether its protective action is extended toward erythrocytes, the first exposed cellular system to various exogenous and endogenous stressors. Moreover, melatonin was also found to exhibit cardio-protection when ISO aggravated high-fat diet-induced oxidative stress-mediated myocardial onslaught. Our studies revealed the association of a unique pathway in cardio-protection by melatonin. These findings further strengthen the role of melatonin as a cardio-protective antioxidant with no or minimal side effects, recognized globally and having immense future therapeutic relevance.

Keywords: Melatonin, antioxidant, ischemic heart disease, myocardial damage, reactive oxygen species, mitochondrial dysfunction, oxidative stress.

Indian Journal of Physiology and Allied Sciences (2023);

DOI: 10.55184/ijpas.v75i02.152

ISSN: 0367-8350 (Print)

INTRODUCTION

The global burden of cardiovascular diseases (CVDs) has increased at an alarming rate with well-developed countries leading in cases related to CVD associated disability and mortality.¹ Reactive oxygen species (ROS) play a critical role in the pathogenesis of various diseases, including cardiovascular injury associated with circulatory disturbance. Recent studies have indicated the involvement of ROS in myocardial ischemia. Myocardial infarction is associated with ischemic necrosis of cardiac muscles due to a decrease in the supply of blood to a portion of the myocardium below a critical level necessary for viability and proper physiological function.² Along with CVDs, Coronary artery disease (CAD) is also significantly increasing in the present population. Consumption of high fat diet (HFD) in different populations has been on the rise for decades due to the currently fast-paced general lifestyle.^{3,4} High fat diet potentiates the development of atherosclerosis by not only depositing cholesterol but also causes injury to endothelium by enhancing the production of free radicals and oxidized LDL.⁵ It was observed that when high fat diet combined with certain pharmacological agents, this combination significantly promotes the severity of CAD in any individual.⁶ Isoproterenol (ISO) being one such agent. Isoproterenol (ISO),

Department of Physiology, Oxidative Stress and Free Radical Biology Laboratory, University of Calcutta, University College of Science and Technology, Kolkata, India

Email: debasish63@gmail.com

How to cite this article: Bandyopadhyay D. Role of melatonin as a protective antioxidant in the amelioration of oxidative stress mediated tissue injury: a new vision for futuristic medicine. *Indian J Physiol Allied Sci.* 2023;75(2):8-20.

Conflict of interest: None

Submitted: 21/02/2023 **Accepted:** 20/03/2023 **Published:** 25/06/2023

a β -adrenergic agonist, causes ischaemic heart disease (IHD) in experimental rats with pathophysiological effects similar to those found in humans.⁷

Mitochondria, the seat of oxidative phosphorylation and energy production, plays a pivotal role in ROS induced oxidative damage to important macromolecules like DNA, proteins and lipids, eventually leading to cellular apoptosis.⁸ The mitochondria's electron transport chain (ETC), the principal source of cellular energy, is also the principal source of free radical generation within a cell. The mitochondrial ETC generates a basal level of reactive oxygen (ROS) and nitrogen (RNS) species under ambient conditions which may multiply several fold under conditions of stress such

as ischaemia/reperfusion, drug or chemical-induced cell damage or external pathogen attack.⁹ The patho-physiology of ischemic heart disease thus involves mitochondrial dysfunction concomitant with the generation of oxidative stress.¹⁰ In our earlier studies, we observed the protective role of melatonin in an *in vivo* rat model where it protected the rat heart myocardium from oxidative damage. Restoration of diminished cardiac function after ISO treatment by melatonin, evident from the rat heart's hemodynamic parameters, clearly indicates its cardio-protective role.² Melatonin ameliorated ISO-induced alterations in the activity of key mitochondrial ETC enzymes as well as aided in myocardial recovery after an ischaemic shock. We have also demonstrated earlier that melatonin pretreatment could significantly reduce the levels of pro-apoptotic proteins indicating a protective role of this small indole against ISO mediated oxidative stress-induced cellular apoptosis.² Since mitochondria is considered the seat of energy metabolism, we have also previously examined the effect of ISO on isolated goat heart mitochondria and provided evidence that ISO caused oxidative stress mediated mitochondrial damage as reflected by elevated lipid peroxidation and decreased glutathione levels. Isoproterenol also competitively inhibited the activity of key mitochondrial ETC enzymes and increased mitochondrial membrane potential which provided a signal to trigger apoptosis.¹¹ Another study reported by us suggests that activation of SIRT1-PGC-1 α -SIRT3 pathway by melatonin along with its biophysical properties, prevented ISO induced mitochondrial injury in rat heart.¹² Melatonin has also efficiently mitigated the altered metabolic parameters induced by high fat diet (HFD) animal models. These parameters included blood glucose, lipid profile, body weight, circulating leptin, adiponectin level, energy expenditure, glucose and fat metabolism.¹³ The mechanistic studies have uncovered that the protective effects of melatonin on the myocardial damage induced by HFD and ISO are attributed to its direct and indirect antioxidative capacity, i.e., it directly scavenges free radicals and also regulates the gene expression of antioxidant enzymes.¹⁴

Melatonin acts via two identified pathways, i.e., receptor-dependent and receptor-independent pathways. Studies suggest two receptor-independent pathways by which melatonin provides protection to antioxidant enzymes against ROS mediated oxidative damage, namely: (i) through the free radical scavenging ability of melatonin and (ii) through the metal chelating property of melatonin to bind to the free, unbound metal ions itself. We confirm that melatonin ameliorated the ISO-induced changes to isolated goat heart mitochondria. We also observed that ISO generated free radicals in this *in-vitro* system and melatonin scavenged the reactants. The ISO- induced mitochondrial damage seemed to be perpetrated exclusively due to the generation of oxidative stress, while melatonin provided protection via its antioxidant mechanisms. We also identified and elucidated a third mechanism by which melatonin

prevents oxidative damage to antioxidant enzymes by the copper-ascorbate system, *in-vitro*, through biochemical analysis in both a cell free/chemical system as well as incubated cellular components (mitochondria, cytosol and peroxisome) and isothermal calorimetric binding studies.¹⁵

MATERIALS AND METHODS

Experiments Involved with Cardiac Tissue

For the *in-vivo* studies, male Wistar rats were used and they were divided into different groups like control, ISO treated, melatonin treated only (positive control) and melatonin pre-treated followed by ISO treatment. The ISO treated rats were given 25 mg ISO/kg body weight (bw) of rats 30 minutes prior to melatonin administration. Different doses (5, 10, 20, 40 mg/kg bw) were used for melatonin to test and evaluate its efficacy against ISO. For experiments with high fat diet (HFD) - 60% of total kcal consumed was composed of fat. After the rats were euthanized following light ether anesthesia, blood was drawn for analysis of serum parameters and the cardiac tissue was collected carefully for the studies of the activity of enzymes and the levels of different proteins. The protocols of the *in vivo* studies had the approval of the Institutional Animal Ethical Committee (IAEC) of the Department of Physiology, University of Calcutta.

Isolation of cardiac mitochondria for *in-vitro* studies: Goat cardiac tissue has been reported to have high mitochondrial content. Thus, goat cardiac tissue was obtained from government registered slaughterhouse. The cardiac tissue was cleaned in ice-cold 0.9% NaCl and homogenized as described earlier.¹⁶ The mitochondria were isolated according to a standard procedure. The isolated mitochondria were stored in sterile vials and either freshly used or stored at -80°C to be used later.

Isoproterenol-induced cardiac mitochondrial injury adose response study: Approximately 6–8 mg/mL of mitochondrial protein was incubated with 0.125, 0.25, 0.5, 1.0, 2.0, 4.0 and 6.0 μ M of ISO bitartrate in lysis buffer for 60 min at 37°C.

Isoproterenol-induced cardiac mitochondrial injury - protection by melatonin: Isolated goat heart mitochondria were incubated with 2 μ M ISO and different concentrations of melatonin (0.125, 0.25, 0.5, 1.0, 2.0, 4.0 μ M) for 60 minutes at 37°C.

Antioxidant enzyme profile: Xanthine oxidase was assayed by measuring the conversion of xanthine to uric acid following the method of Greenlee and Handler (1964).¹⁷ Western blot analysis was performed with left ventricular (LV) tissue homogenates that were prepared as described earlier by Bandyopadhyay *et al.* (2004)¹⁸ with minor modifications. Measurement of free hydroxyl radical (\cdot OH), superoxide anion free radical, protein carbonylation and inducible nitric oxide synthase (iNOS) activity, reduced glutathione, oxidized glutathione and redox potential, lipid peroxidation, mitochondrial Mn-superoxide dismutase and glutathione

peroxidase, activities of the mitochondrial Krebs' cycle and respiratory chain enzymes were measured according to the methods mentioned earlier.^{2,11} Triglyceride, total cholesterol, HDL cholesterol and LDL cholesterol were estimated in serum by using a commercial kit purchased from Arkray healthcare Pvt. Ltd. (India). Kit instructions were strictly followed to perform the tests and calculations were done by the instruction provided with the kit where Friedewald's equation was used to estimate LDL cholesterol.

Mitochondrial status in presence and/or absence of isoproterenol and mitochondria: Mitochondrial membrane potential was determined by using the mitochondria-specific lipophilic cationic fluorescent dye JC-1 following a well calibrated method of Cossarizza *et al.* (2000).¹⁹ The flow cytometer (BDFACS Versa, USA), with the excitation wavelength 488 nm and an emission wavelength of band pass filter 586/42 nm was used for the detection of mitochondrial membrane potential ($\Delta\psi_m$) and the FITC-A median was expressed as depolarized population percentage (%).

In search of mechanism of action of melatonin apart from its conventional actions: For further *in-vitro* and cell-free experiments, 60% cytosolic, 60% peroxisomal and 50% mitochondrial suspension isolated from goat hearts was taken in 50 mM potassium phosphate buffer and was incubated at 37°C (pH 7.4) in five different groups each containing graded concentrations of: (i) CuCl_2 (0.04, 0.08, 0.1 and 0.2 mM), (ii) ascorbic acid (0.2, 0.4, 0.8 and 1 mM) (iii) ascorbic acid (0.2, 0.4, 0.8 and 1 mM) in combination with a fixed concentration of CuCl_2 (0.2 mM) (iv) melatonin (0.125, 0.25, 0.5 and 1 μM) in the presence of 0.2 mM CuCl_2 and 1 mM ascorbic acid (except peroxisomal samples where different set of melatonin concentrations were used, such as 10, 20, 40 and 80 μM). We also incubated pure Cu-Zn SOD (SOD-1) at a concentration of 0.1 mg/mL following the same incubation protocol as mentioned above in a cell free medium/chemical system to compare the findings with those obtained in the *in-vitro* experiments. The binding pattern of pure Cu-Zn superoxide dismutase (SOD-1) with copper chloride, ascorbic acid, copper-ascorbate system and melatonin was also analysed by isothermal titration calorimetry using Microcal ITC-200, Malvern, UK. For a single run, titration was conducted with twenty injections of each ligand (2 μL each) with 150 s spacing between two successive injections for approximately 1-hour at 37°C.²⁰

Experiments Involved with Gastric Tissue

Induction of stress ulcer: Fasted (water ad libitum) Wistar rats (220–250 g) of the cold-restraint stress group were immobilized in a supine position under light ether anesthesia and were kept for 3.5 hours to induce gastric ulcers. Fasted animals of the non-stressed control group were exposed to ether and kept at room temperature without stress. The animals of the drug-treated group were injected with melatonin, ranitidine, or omeprazole i.p., 30 minutes before the onset of the stress. The cold-restraint stress group

received the same amount of vehicles. In experiments where melatonin was used in combination with ranitidine or omeprazole, drugs were injected i.p. 15 min before melatonin administration.

Piroxicam-induced gastric ulceration and protection by melatonin: Gastric ulcers were induced in rats by oral administration of piroxicam. In brief, fasted (water ad libitum) Wistar rats. (220–250 g) were divided into three groups. The rats of the first group served as vehicle-treated control. The rats of the second group were fed orally with different doses of piroxicam (5.0, 7.5, 10.0, 20.0 and 30.0 mg/kg). To the third group, melatonin (60 mg/kg) [dissolved in not more than 10% ethanol] was injected i.p. 30 min before piroxicam administration. The animals were kept at room temperature and were sacrificed after 4 hr to assess the degree of gastric lesion.

Ulcer Index measurement: Gastric ulcers were induced in rats by restraint-cold stress, and the damage's severity was expressed as the ulcer index (MUI). The grade of lesions was scored following the scale: 0, no pathology; 1, small 1–2 mm ulcers; 2, medium 3–4-mm ulcers; 4, large 5–6 mm ulcers; 8, ulcers greater than 6 mm. The sum of the total ulcer score in each group of rats divided by the number of animals.²¹

Western blot analysis: A portion of the fundic stomach was homogenized in 50 mM phosphate buffered saline (pH 7.4) and centrifuged at 5000 g for 10 min. The supernatant was resolved by 10% sodium dodecyl sulphate-polyacrylamide gel electrophoresis (SDS-PAGE) according to Laemmli's method using Mini Protean II apparatus (Bio-Rad Laboratories, Hercules, CA, USA). Fifteen, 25, 30, and 50 μg proteins were loaded for immunodetection of Cu, Zn-SOD, catalase, alpha-actinin and COX-1, respectively. After SDS-PAGE, proteins were transferred onto polyvinylidene difluoride membranes (ImmobilonTM-P, Millipore Corporation, Bedford, MA, USA) in an electro-blotting apparatus (Mini Trans-Blot, Bio-Rad) at 90 V using 193 mm glycine, 25 mm tris, 20% methanol as transfer buffer. After transfer, membranes were blocked using 5% nonfat dried milk in Tris-buffered saline containing 0.05% Na-azide (pH 7.6), and incubated for 2 hours at room temperature. The membranes for Cu, Zn-SOD, catalase, alpha-actinin and Cox-1 were rinsed twice with tris-buffered saline (pH 7.6) containing 0.1% Tween 20 (TBS-T), and then incubated with respective primary antibody (1:2500; 1:2000; 1:2500 and 1:1000 dilutions, respectively) overnight. After washing thrice with TBST, membranes were incubated in secondary antibody for 4 hr at room temperature, followed by a further washing with TBST. The immunoreactive bands were detected using in the presence of nitro blue tetrazolium-5-bromo-4-chloro-3-indolyl phosphate (NBT-BCIP; Sigma-Aldrich Co., St. Louis, MO, USA) (2:1). The density of bands obtained through Western blotting was quantified with ImageJ software.

Study of gastric tissue using combination of physiological molecules: Male Wistar rats (n=24), were randomly divided into 4 groups. The control group were injected (s.c.) with vehicle, while rats in the other groups were injected (s.c.) with

0.125 (AD1), 0.25 (AD2) and 0.50 (AD3) mg/kg of adrenaline bitartrate (AD), respectively for 15 days at 12:30 h. Male Wistar rats (n=48) were divided into 8 groups. Control group were injected (s.c.) with vehicle, while rats in the second group was injected (s.c.) with 0.25 mg/kg of AD. The 3rd – 5th groups were orally (gavage) given different doses of melatonin (2.5, 5.0, 10.0 mg/kg, respectively). Rats in the 6th- 8th groups were given different doses of melatonin daily (2.5, 5.0, 10.0 mg/kg, respectively) 30 min prior to AD injection. The treatment was carried out for 15 consecutive days. Melatonin solution (40 mg/mL) was prepared daily in ethanol and saline (0.9%) mixture (1:9) in amber container to avoid its light induced degradation. Animals were treated with melatonin at 12:00 h corresponding to the highest concentration of daily melatonin in the stomach, as melatonin levels in the different gastrointestinal tissues is known to have no significant diurnal variation.²²

Measurement of melatonin concentration in GI tissues: Concentration of melatonin in the gastrointestinal tissue homogenates were measured following the manufacturer's instructions of a rat MT (Melatonin) ELISA kit (ER1169; Wuhan Fine Biotech Co., Ltd., Wuhan, China).

Tissue levels of pro- and anti-inflammatory cytokines: Levels of pro-inflammatory (IL-1 β , IL-6 and TNF α) and anti-inflammatory (IL-10) cytokines in the tissues were estimated following the manufacturer's (RayBiotech, Norcross, GA) instructions. In brief, 100 μ L samples were added to each well and incubated for 2.5 hours at room temperature (RT), then, the solution was discarded and wells were washed 4 times in washing buffer. Then, 100 μ L of biotinylated antibody were added to each well and again incubated for 1-hour at RT. After discarding the solution, wells were again washed in the same manner. 100 μ L of streptavidin solution were added to each well and incubated for 45 minutes at RT. Again, the solution was discarded and the wells were washed, then 100 μ L of TMB substrate reagent were added to each well and incubated for 30 minutes at RT under complete dark condition. Finally, 50 μ L of stop solution was added to each well and the reading was immediately recorded at 450 nm. All reagents were prepared strictly following the manufacturer's instructions.

Assessment of tissue architecture by histology and scanning electron microscopy (SEM): Paraformaldehyde (4%) fixed gastrointestinal tissues were embedded in paraffin and sliced to 5 μ m thick sections which were further deparaffinized and stained with hematoxylin-eosin (HE) to identify tissue morphology. Similar deparaffinized slides were used to stain the cell nuclei with 4', 6'-diamino-2-phenylindole (DAPI; 1 μ g/mL) for the morphological assessment of the apoptotic cells following the method of Mohankumar *et al.*²³ Stomach, duodenum and colon tissue sections were subjected to SEM analysis following the technique of Cheema and Scofield²⁴ and observed under a scanning electron microscope (SEM; Zeiss Evo 18 model EDS8100) available at CRNN, University of Calcutta, India.

Analysis of apoptosis in different gastric tissue sections:

Deparaffinised slides were used to stain the cell nuclei with 4', 6'-diamino-2-phenylindole (DAPI; 1- μ g/mL) for the morphological assessment of the apoptotic cells following the method of Mohankumar *et al.*²³

Experiments Involved with Erythrocytes Preparation of Whole Erythrocytes From Goat Blood

Goat blood was carefully collected from slaughter house sanctioned by local Kolkata Corporation in citric acid-dextrose buffer. Packed cells (RBCs) were obtained by centrifugation at 3000 rpm for 10 minutes. The plasma (supernatant) and the buffy coat were removed by aspiration and the whole RBCs, the packed cells, were washed thrice with 0.9% NaCl solution.

Determination of the optimally effective concentration of melatonin against PHZ induced oxidative stress in RBCs

***in-vitro*:** The RBCs were incubated with PHZ (1 mm) and/or different concentrations of melatonin. The treated groups are as follows: Group I: Control (CON) without any treatment; Group II: PHZ treated group (PHZ); Group III: PHZ + melatonin (5 nmoles/mL) (PM5); Group IV: PHZ + melatonin (10 nmoles/mL) (PM10); Group V: PHZ + melatonin (20 nmoles/mL) (PM20); Group VI: PHZ + Melatonin (40 nmoles/mL) (PM40).

Measurement of metabolic enzymes: The activities of hexokinase, phosphofructokinase, G6PDH, aldolase and lactate dehydrogenase activities were determined from RBC hemolysate and all activities were expressed as units/mg protein.

Scanning Electron Microscopy: Control and treated groups of RBCs were fixed using 3% glutaraldehyde and the images were captured using a Scanning Electron Microscope available at CRNN facility of University of Calcutta.

Statistical analysis: Each experiment was repeated at least three times. Data are represented as mean \pm S.E.

RESULTS

Treatment of rats with ISO caused alterations in the levels of biomarkers of oxidative stress, activities of antioxidant enzymes as well as some of the Krebs' cycle enzymes significantly which all were found to be ameliorated when the rats were pre-treated with melatonin at a dose of 10 mg/kg bw. The results also reveal that pre-treatment with melatonin provided cardioprotection.

Figure 1 indicates how ISO administration to rats induced the generation of ROS. The results presented in Figure 1A–E clearly indicate that there was an enhancement in the generation of O₂⁻ *in vivo* following treatment of rats with ISO. The activities of xanthine oxidase (XO), xanthine dehydrogenase (XD), total enzyme activity, that is, XO plus XD, XO

- XD ratio and XO/XO + XD ratio all increased significantly following ISO treatment of rats. All these parameters were restored to normal levels when the rats were pre-treated with melatonin, indicating melatonin's ability to neutralize free radicals *in vivo*.

Figure 2(A) shows an ISO-induced elevation ($p < 0.001$ versus control) of the apoptotic protease activating

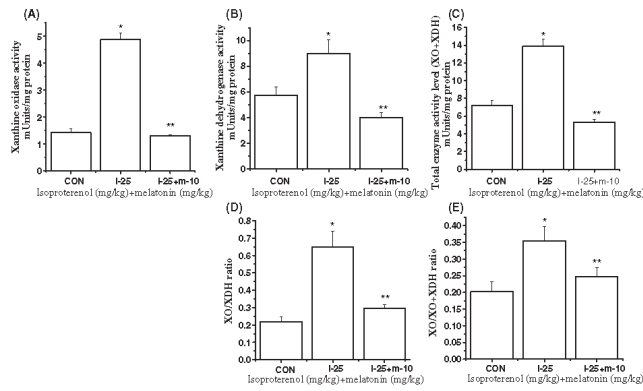


Figure 1: Protective effect of melatonin against ISO-induced increase in the activities of (A) xanthine oxidase and (B) xanthine dehydrogenase in control (CON), ISO- treated (I), and melatonin (m) protected rats. Values are mean \pm S.E.M. of eight rats in each group. * $P < 0.001$ versus CON, ** $P < 0.001$ versus I. (C) Total enzyme activity (XO + XDH), (D) xanthine oxidase/xanthine dehydrogenase (XO/XDH) ratio, (E) xanthine oxidase/xanthine oxidase + xanthine dehydrogenase (XO/XO + XDH) ratio. (Published in Mukherjee *et al.* Journal of Pineal Research, 2010)²

factor 1 (Apaf-1), the protein involved in the formation of apoptosome complex with cytochrome c that cleaves Procaspase 9 to its activated form. This ISO-induced elevation of Apaf-1 level is decreased significantly by melatonin ($p < 0.001$ versus I). Figure 2(B) shows the significant elevation of the level of activated Caspase 9, the protein involved in cellular apoptosis, by ISO ($p < 0.001$ versus control) and its amelioration by melatonin ($p < 0.01$ versus I).

The fact that ISO damages the mitochondria through the induction of oxidative stress is evident from Figure 3(A–C) which shows a dose- and time-dependent increase in mitochondrial lipid peroxidation level *in-vitro* which are then dose dependently protected by melatonin. The dose-dependent studies indicated that the dose of 2 μ M for ISO and 1 μ M (final concentrations, respectively) for melatonin as the minimum effective doses and incubation time of 60 min as the optimum. This ISO-induced induction of oxidative stress results in a change in mitochondrial redox status as evident from Figure 3 (D, E) which shows significant decrease in the GSH/GSSG ratio (Figure 3D) along with alteration in mitochondrial redox potential (Figure 3E) upon ISO (2 μ M)-incubation and concomitant recovery on co-incubation with melatonin (1 μ M). Figure 3(F) depicts reciprocal alteration in the activities of cardiac mitochondrial antioxidant enzymes, like, Mn-SOD and glutathione peroxidase (GPx) with Mn-SOD showing 56% increase in activity with ISO (2 μ M)-incubation which is recovered to almost control level on melatonin (1 μ M) co-incubation, while GPx shows significantly decreased activity on ISO treatment which is significantly ameliorated by melatonin. Incubation of the cardiac mitochondria with melatonin alone (positive control) did not show any alteration in the enzyme activities.

The values of triglycerides, total cholesterol, LDL-c, HDL-c and the ratios of total cholesterol: HDL-c and LDL-c: HDL-c is

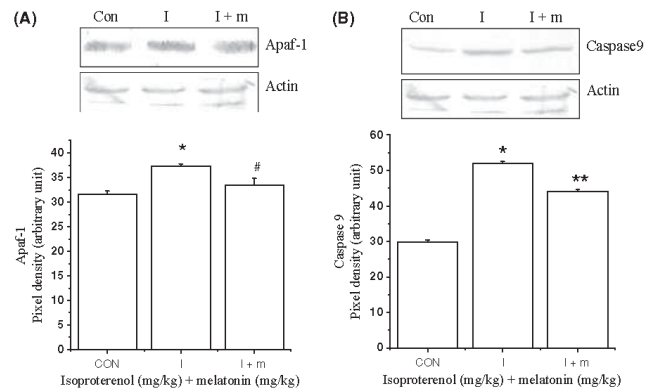


Figure 2: (A) Representative result of Western blot analysis for determining the level of apoptotic protease activating factor (Apaf)-1 (lanes from left) of heart tissue in control(CON),ISO-treated (I), and melatonin (m)-protected rats. The Western blot analysis was repeated at least three times. Actin served as loading control. The pixel density of bands obtained through Western blotting was quantified with ImageJ software (NIH), and the values (mean \pm S.E.M.) were presented below in the form of a bar graph. * $P < 0.001$ versus CON; # $P < 0.001$ versus I. (B) Representative result of Western blot analysis for determining the level of caspase 9. Actin served as loading control. The pixel density of bands obtained through Western blotting was quantified with ImageJ software (NIH), and the values (mean \pm S.E.M.) were presented in the form of a bar graph. * $p < 0.001$ versus CON; ** $p < 0.01$ versus I. (Published in Mukherjee *et al.*, Journal of Pineal Research, 2012)¹¹

shown in table 1. The values of all parameters (except of the HDL-c) were significantly increased in the rats treated with H, I and HI compared to the control, respectively. The highest value was observed in the group of HI. Melatonin at the dose of 40 mg/kg bw significantly protected these parameters from being altered in H, I and HI treatment group. In contrast, the value of HDL-c was significantly reduced in rats treated with H, I and HI compared to the control group, respectively. However, melatonin at the dose of 40 mg/kg bw brought this value back to the control level.

Flow cytometric analysis of JC-1 stained mitochondria revealed that majority of control mitochondria are polarized (Figure 4A). However, ISO-treated mitochondria showed predominantly depolarized populations. Surprisingly, mitochondria from melatonin pre-treated group showed a significantly lower percentage of depolarized population as illustrated in figure 4B.

The isothermal titration calorimetry (ITC) graphs that show the interaction of copper with melatonin as well as ascorbic acid with melatonin is shown in Figure 5, where we observed that both interactions occur at single sites. However, heat change per second is more rapid and higher in case of ascorbic acid, melatonin and SOD group (Figure 5B) than copper, melatonin and SOD group (Figure 5A) as inferred by the area under the curve. Upon titration of SOD with a combination of both these ligands (copper and ascorbate), a prominent exothermic heat change along with a strong affinity binding was observed (area under the curve), which reached to saturation level progressively with time (Figure

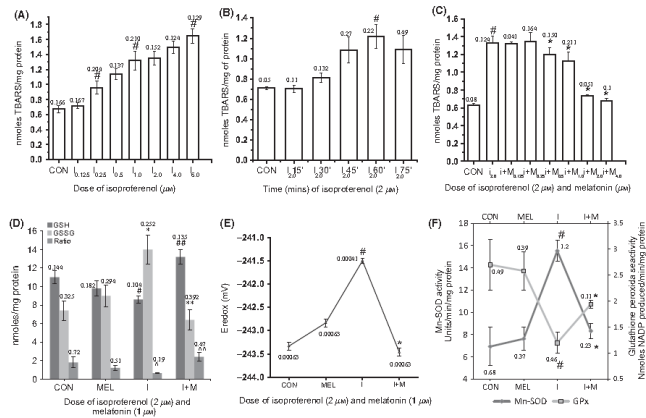


Figure 3: Changes in mitochondrial lipid peroxidation levels on incubation with (A) increasing doses of isoproterenol (ISO). A total of 2 μM (final concentration) was taken as the minimum effective dose; (B) 2 μM (final concentration) ISO for different time points. A total of 60 min was taken as the optimum incubation time. (C) Lipid peroxidation level of isolated goat heart mitochondria incubated with 2 μM ISO and different doses of melatonin (MEL). Control (CON) samples were incubated with buffer only. Values are mean ± S.E. for six samples. Numerical values above error bars indicate coefficients of variation. #P < 0.001 versus C; *p < 0.001 versus ISO 2 μM; limit of detection (LOD) for lipid peroxidation (LPO) measurement assay is 0.075. (D) ISO-induced decrease in reduced glutathione (GSH), increase in oxidized glutathione (GSSG), and decrease in GSH/GSSG ratio of isolated goat heart mitochondria and amelioration by melatonin. Control (CON) samples were incubated with buffer only. Positive control samples are incubated with melatonin (MEL) only. Values are mean ± S.E.M. for six samples. Numerical values above error bars indicate coefficients of variation. #P < 0.001 versus C; #*,^# p < 0.001 versus ISO 2 μM; LOD is 1.02. (E) Decrease in mitochondrial redox potential on incubation with 2 μM ISO (final concentration) for 60 minutes *in-vitro*. Co-incubation with 1 μM melatonin (MEL) recovered the membrane potential to control level. Control (CON) samples were incubated with buffer only. Positive control samples were incubated with melatonin (MEL) only. Values are mean ± S.E. for six samples. Numerical values above/below error bars indicate coefficients of variation. #P < 0.001 versus C; *p < 0.001 versus ISO 2 μM; (F) Isoproterenol (ISO)-induced increase in mitochondrial Mn-superoxide dismutase (Mn-SOD or SOD2) activity and decrease in glutathione peroxidase (GPx) activity *in-vitro* and protection by melatonin (MEL). Mitochondria were incubated with 2 μM ISO with or without 1 μM melatonin for 60 minutes. Control (C) samples are incubated with buffer only. Positive control samples are incubated with melatonin (MEL) only. Values are mean ± S.E. for six samples. Numerical values above/below error bars indicate coefficients of variation. #P < 0.001 versus C; *p < 0.001 versus ISO 2 μM. (Published in Mukherjee *et al.*, Journal of Pineal Research, 2015)²⁵

5C). Ultimately in case of titration of SOD in the presence of melatonin in combination with CuCl₂ and ascorbic acid in the ligand cell, it showed a sequential binding pattern of ligands with multiple binding sites, however, delay in saturation with time was significantly observed (Figure 5D). Figure 6A shows that melatonin dose-dependently protected the mucosa from stress-induced ulceration, causing a 87% inhibition of the ulcer index when the indole was given at a dose of 60 mg/kg BW (i.p.). The effect of melatonin was compared with two already marketed antiulcer drugs, i.e. ranitidine and omeprazole, in protecting against stress induced gastric ulceration. Both drugs were found to reduce

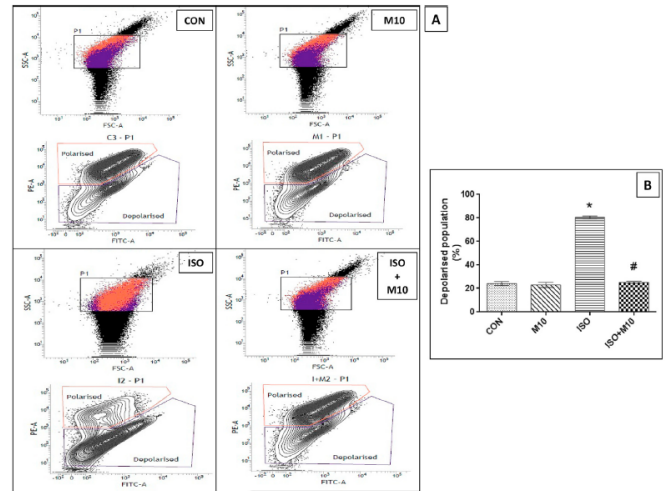


Figure 4: Fluorometric analysis of rat heart mitochondria following JC-1 staining. Panel (A) shows the FACS distribution pattern of cardiac mitochondria stained with JC-1 dye according to change in membrane potential of the different groups, i.e., control (CON), melatonin only (MEL10), ISO treated (ISO) and ISO + melatonin treated (ISO + MEL10) group. Panel (B) represents the histogram showing the fluorescent intensity (%) of JC-1 (percent of depolarized population of mitochondrial membrane) of the different groups. Values are expressed as mean ± S.E. for six samples for each group. (*p < 0.001 versus control, #p < 0.001 versus ISO treated heart, using one way ANOVA). (Published in Naaz *et al.*, Heliyon, 2020)¹²

stress ulceration dose-dependently. At lower doses, however, melatonin appears to be a better gastroprotective agent than ranitidine, with omeprazole being the most effective. Figure 6B, C show a remarkable protection of the mucosa from stress ulceration when melatonin, along with ranitidine or omeprazole, was injected i.p. into animals at the minimum doses at which none of the drugs were effective in protecting against stress-induced ulceration individually.

Figure 7A reveals that melatonin dose-dependently protected the mucosa from piroxicam-induced gastric ulceration, causing a 92% inhibition of the ulcer index when the indole was given at a dose of 60 mg/kg BW (i.p.). Four hours after oral administration of piroxicam (30 mg/kg BW), severe hemorrhagic ulcer spots were evident as shown in Figure 7B (1 and 2) is the stomach of a control rat with no hemorrhagic ulcer. On pretreatment of the animals with melatonin (60 mg/kg, i.p.) in piroxicam fed group, few hemorrhagic ulcer spots were detectable on the inner mucosal surface [Figure 7B (3)].

A rise in the catalase protein level was evidenced from western blot analysis in the piroxicam-treated animals compared with controls. While melatonin restored catalase activity to near normal values, it did not have a significant inhibitory effect on catalase expression (Figure 8A). The enhanced Cu-Zn-SOD activity in the piroxicam treated group may be due to enhanced synthesis of the respective protein as is evident from the western blot analysis (Figure 8B). Pretreatment of the rats with melatonin further increased the level of Cu-Zn-SOD. Figure 8C reveals that piroxicam treatment (30 mg/kg BW, orally) significantly

Table 1: Effects of melatonin on the concentrations of triglyceride, total cholesterol, LDLc, HDL-c, LDL:HDL and total cholesterol:HDL-c in serum of rats treated with high fat diet (H), isoproterenol (I) and high fat diet and isoproterenol (HI), respectively. Values are expressed as mean \pm S.E.M. (N = 6). * $p < 0.001$ versus C, $\wedge p < 0.001$ Vs H, $\sim p < 0.001$ Vs I, # $p < 0.001$ Vs HI. (Published in Ghosh *et al.*, Melatonin Research, 2019)¹⁴

Groups	Hydroxyl radical nmoles MSA/mg protein	Mean Fluorescence Intensity (Arbitrary Unit)			
		Mitochondrial fraction		Cytosolic fraction	
		Di- tyrosine	Tryptophan	Di-tyrosine	Tryptophan
C	90.1 \pm 0.36	33.4 \pm 2.01	373.7 \pm 34.54	52.8 \pm 0.79	432.7 \pm 16.15
M40	84.4 \pm 7.63	34.0 \pm 0.40	377.0 \pm 15.01	53.0 \pm 0.63	434.4 \pm 37.29
H	154.5 \pm 4.58*	46.4 \pm 2.81*	247.2 \pm 24.85*	64.2 \pm 1.79*	266.5 \pm 15.70*
HM40	90.2 \pm 2.33 \wedge	31.2 \pm 0.14 \wedge	373.6 \pm 1.75 \wedge	53.7 \pm 0.88 \wedge	444.6 \pm 18.46 \wedge
I	179.1 \pm 4.95*	53.3 \pm 1.93*	195.5 \pm 14.09*	67.8 \pm 3.37*	249.1 \pm 15.62*
IM40	90.5 \pm 5.34 \sim	33.9 \pm 1.87 \sim	371.1 \pm 19.79 \sim	51.8 \pm 0.17 \sim	415.1 \pm 37.48 \sim
HI	225.8 \pm 4.91* $\wedge\sim$	62.4 \pm 0.83* \wedge	97.3 \pm 5.81* $\wedge\sim$	82.5 \pm 1.61* $\wedge\sim$	117.7 \pm 5.47* $\wedge\sim$
HIM40	107.1 \pm 12.26#	36.1 \pm 1.10#	371.8 \pm 21.39#	53.7 \pm 0.63#	399.2 \pm 10.81#

reduced COX-1 expression which is partially restored on pretreatment of the rats with melatonin (60 mg/kg BW, i.p.). The fact that cellular architecture of the gastric mucosal tissue is damaged in piroxicam-treated animals is revealed in the results presented in Figure 8D. The level of α -actinin, a cellular architectural protein of the mucosal tissue, was significantly reduced in piroxicam-treated animals when compared with its level in control stomach. Pretreatment of rats with melatonin restored the level of α -actinin following piroxicam administration similar to that in control animals. The expression of α -actinin, however, was also slightly

elevated in the rats pre-treated with melatonin. GI tissues had normal cellular architectures in control and melatonin alone groups (Figure 9). However, AD (0.25 mg/kg) treatment distorted the gastric mucosae and lamina propria in the stomach tissue and caused desquamation of the villi tips, accumulation of neutrophils, thus reducing the thickness of the mucosa layer of the villi in duodenum and colon. Melatonin (5 mg/kg) pretreatment treatment

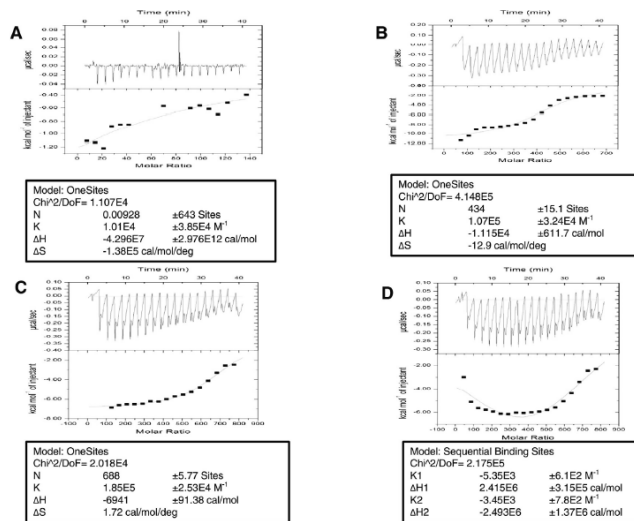


Figure 5: A representative isothermal titration calorimetric dataset of pure superoxide dismutase (SOD). In the heat change vs. time titration curve, each peak represents an injection of ligand into the sample cell that contains pure SOD, where the ligand used is (A) copper chloride and melatonin, (B) ascorbic acid and melatonin (C) copper chloride and ascorbic acid and (D) copper chloride, ascorbic acid and melatonin. The amount of heat change per second (ΔH) is represented by the area under the curve (top curve) and the heat change in terms of kcal mol⁻¹ of injectant against molar ratio is shown in bottom curve of each figure, respectively. Values of ΔH , ΔS and number of sites were expressed in terms of mean \pm S.E. (Published in Ghosh *et al.* Life Sciences, 2017)¹⁵

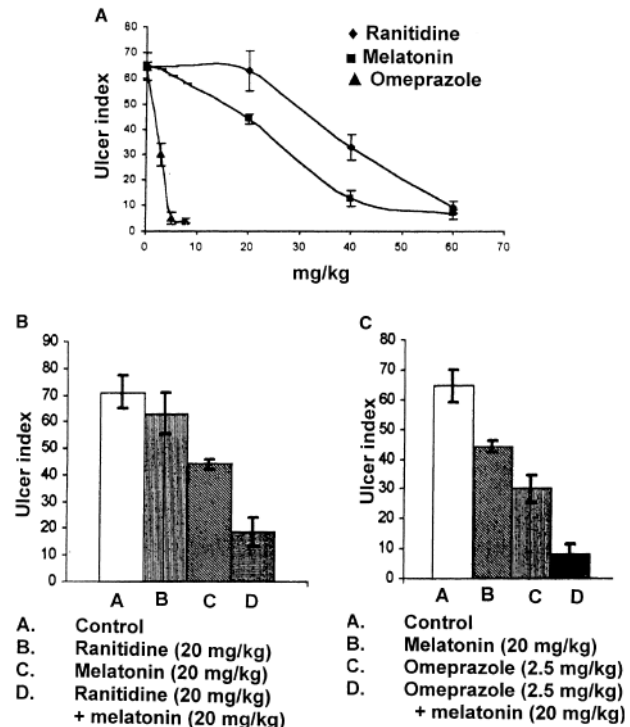


Figure 6: (A) Comparison of the dose-response relationship of melatonin with already marketed antiulcer drugs in restraint-cold stress-induced gastric ulceration. Values are mean \pm S.E.M. of 10 animals. (B) Antiulcer effect of ranitidine and melatonin in combination at the minimum dose. (C) Antiulcer effect of omeprazole and melatonin in combination at the minimum dose. (Published in Bandyopadhyay *et al.*, Journal of Pineal Research, 2002)²⁶

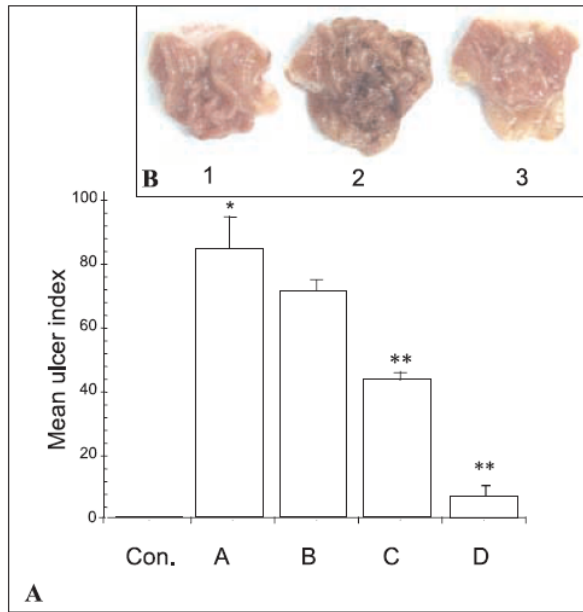


Figure 7: (A) Dose-dependent protection by melatonin against piroxicam-induced gastric mucosal ulceration (expressed as mean ulcer index). Values are mean \pm S.E.M of 10 animals. * $p < 0.001$ versus control, ** $p < 0.001$ versus piroxicam-treated animals. (B) Representation of mucosal surface of the rat stomach in (1) control, (2) piroxicam (30 mg/kg BW)-treated, and (3) piroxicam treated animal pre-treated with melatonin (60 mg/kg BW). Details are in the text. Con., control (no piroxicam); A, piroxicam (30 mg/kg); B, piroxicam (30 mg/kg) + melatonin (20 mg/kg); C, piroxicam (30 mg/kg) + melatonin (40 mg/kg); D, piroxicam (30 mg/kg) + melatonin (60 mg/kg). (Published in Bandyopadhyay *et al.*, Journal of Pineal Research, 2004)¹⁸

preserved the gastric mucosal cells with morphological alterations caused by AD. Moreover, no sign of neutrophil accumulation or, desquamation of the villi neutrophil accumulation or, desquamation of the villi or, damage in the lamina propria layer or, damage in the lamina propria layer was noted following melatonin pretreatment.

The GI tissues exhibited normal sub cellular structures in the control and melatonin alone groups under the SEM observation (Figure 10). However, AD (0.25 mg/kg) treatment caused stomach mucosal injury, and apical cellular erosion of the microvilli in the duodenum and colon tissues (Figure 10). Moreover, breakage of the villi tip was widely present in the duodenum and mucosal surface in the colon tissues leading to loss of tissue integrity. Melatonin treatment protected the AD induced GI tissue damages and there was no erosion in the lamina propria as well as villus tip; thus epithelial cells were found to be almost intact in all three GI tissues with melatonin pretreatment (Figure 10). The results are consistent with DAPI staining which showed apoptotic changes in GI tissues treated with AD. These changes included enhancement in the fluorescence along with frequent chromatin condensation in the nuclei of the epithelial cell distributed at the tip of the microvilli and lamina propria and partially denuded epithelium of villi. All changes were also prevented by melatonin pre-treatment (Figure. 11).

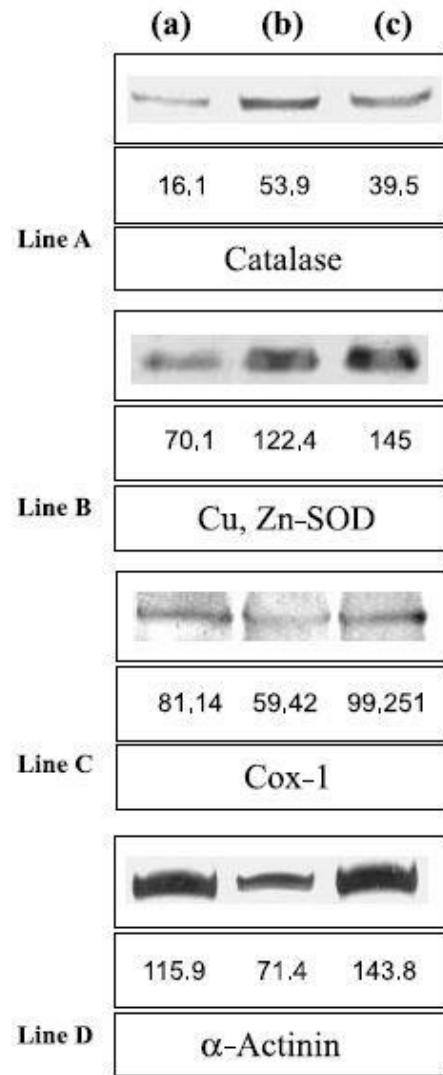


Figure 8: Representative results of Western blot analysis for determining the levels of gastric catalase, Cu-Zn-SOD, COX-1 and a-actinin in control, piroxicam treated as well as melatonin protected rats. In each case, lane (a) represents control, lane (b) piroxicam treated, and lane (c) melatonin plus piroxicam treated. The Western blot analysis for each protein was repeated at least three times. (A) Catalase, (B) Cu-Zn-SOD, (C) COX-1, (D) a-actinin. The pixel density of bands obtained through Western blotting was quantified with ImageJ software (NIH, USA) and the values were presented below the respective band. (Published in Bandyopadhyay *et al.*, Journal of Pineal Research, 2004)¹⁸

Concentration s of melatonin and relative abundance of AANAT and MT1 (Figure 12 in stomach, duodenum and colon tissues were significantly ($p < 0.001$) decreased in AD (0.25 mg/kg) treatment but increased in melatonin alone group compared to control. However, melatonin (5 mg/kg) pretreatment significantly $p <$ preserved the levels of melatonin which was depleted by AD treatment. In addition, the expression of AANAT and MT1 was up-regulated in GI tissues of AD+M group compared to AD (Figure 12).

The activities of G6PDH, hexokinase, phosphofructokinase and aldolase were reduced by 98.09, 48.68, 22.86 and 60.56%

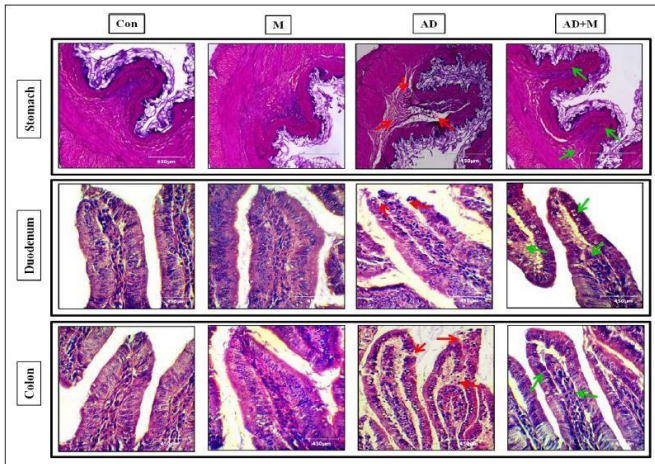


Figure 9: Representative images of HE staining of rats' stomach, duodenum and colon tissues. All the tissues exhibited normal cellular architecture in the control and melatonin treated groups. AD treatment caused profound cellular distortions (red arrows) in the mucosa and lamina propria along with desquamation of the epithelial lining. Melatonin pretreatment prevented these alterations in the concerned tissues (green arrows). Con: control, M: melatonin 5mg/kg, AD: adrenaline 0.25 mg/kg. AD + M: adrenaline + melatonin. (Published in Pal *et al.*, Melatonin Research, 2020)²⁷

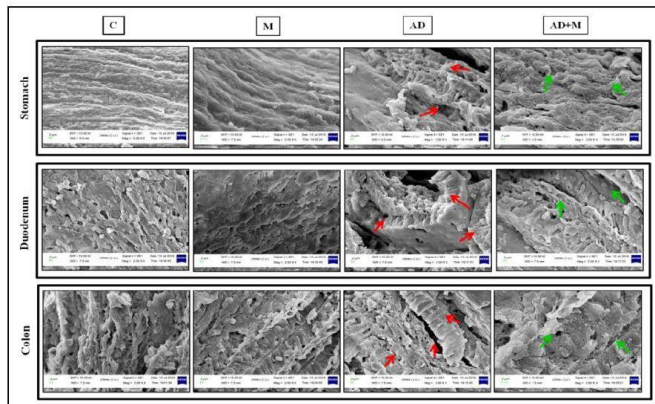


Figure 10: Representative images of scanning electron microscopic (SEM) study of rats' stomach, duodenum and colon tissues. All the tissues exhibited normal cellular architecture in the control and melatonin treated groups. AD treatment caused structural damages (red arrows) in the mucosa and lamina propria of the gastrointestinal tissues. Melatonin pretreatment prevented these alterations (green arrows) in the concerned tissues. Con: control, M: melatonin 5 mg/kg, AD: adrenaline 0.25 mg/kg. AD + M: adrenaline + melatonin (0.25 mg/kg). (Published in Pal *et al.*, Melatonin Research, 2020)²⁷

respectively, with PHZ treatment compared to the control ($*p \leq 0.001$). In contrast the activity of LDH increased 50% after treatment vs control ($*p \leq 0.001$). These alterations of enzyme activities were completely preserved by melatonin treatment (40nmol/mL) (Figure 13A). The kinetics of G6PDH, i.e., Vmax and Km, were analyzed using LBDR plot. It indicated that the Vmax of G6PDH was significantly decreased; however, the Km was not influenced by PHZ treatment. Melatonin treatment preserved the Vmax of G6PDH of RBCs (Figure

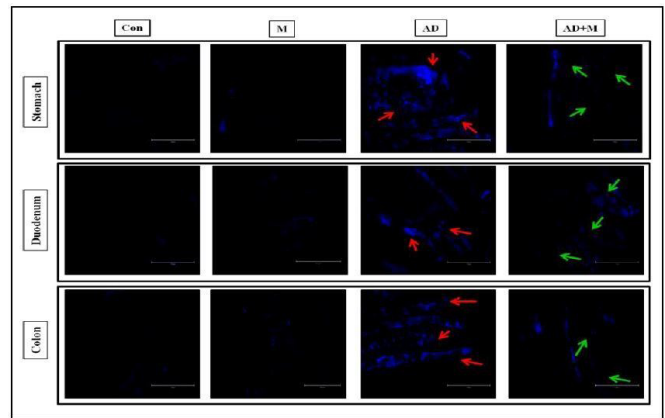


Figure 11: Representative fluorescence photomicrographs of DAPI staining of the stomach, duodenum and colon tissues of rats treated with melatonin and adrenaline. In the control or melatonin alone group, there was no sign of apoptosis-specific morphological changes. AD treatment caused partial denudation of the epithelial lining of the villi and enhanced fluorescence in the nuclei of the epithelial cell distributed at the tip of the microvilli and lamina propria (red arrows). Melatonin pretreatment prevented these apoptotic changes in the concerned tissues (green arrows). Con: control, M: melatonin 5 mg/kg, AD: adrenaline 0.25 mg/kg. AD + M: adrenaline + melatonin (0.25 mg/kg). (Published in Pal *et al.*, Melatonin Research, 2020)²⁷

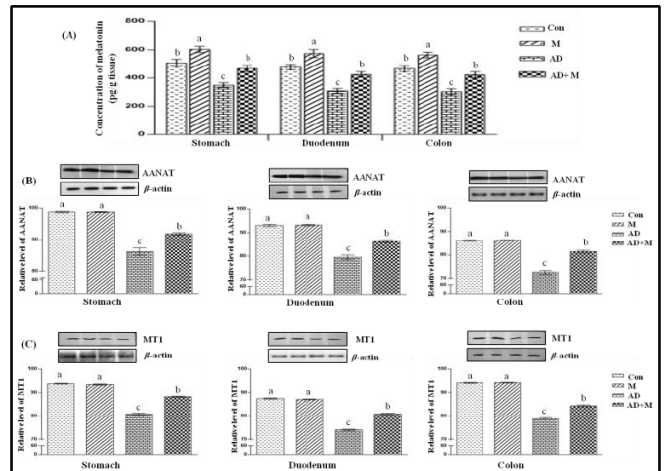


Figure 12: Diagrammatic representation of the (A) melatonin tissue levels, and immunoblots and alterations in the relative densities of (B) arylalkylamine N-acetyl transferase (AANAT) and (C) melatonin receptor 1 (MT1) proteins. Different letters on the error bars indicated significant differences vs each other ($p < 0.001$; $n = 6$ /group), M: melatonin 5 mg/kg, AD: adrenaline 0.25 mg/kg, AD + M: adrenaline + melatonin. (Published in Pal *et al.*, Melatonin Research, 2020)²⁷

13B). The results also showed that both the Vmax and Km of hexokinase were significantly reduced by PHZ treatment and again, melatonin treatment completely reversed these alterations caused by the PHZ (Figure 13C). melatonin alone did not modify these parameters (Figure 13B and C).

The morphology of RBCs was assessed using SEM and the results were shown in Figure 14. Untreated RBCs appeared as typical discocytes while RBCs exposed to PHZ (1mm) exhibited significant change in the cell shape with distinct

echinocyte formation. The morphological changes induced by PHZ (1mm) were greatly prevented when the cells were co-incubated with melatonin (40 nmoles/mL).

The concentrations of Cd in the cardiac, hepatic and renal tissues were significantly ($p < 0.001$) increased in the rats treated with CdCl₂ (Figure 15). Pretreatment with melatonin (10 mg/kg BW.) significantly reduced the Cd loads in heart, liver and renal tissues by 56.44, 31.84 and 44.54%, respectively (Figure 15).

ITC data chart depicts the binding pattern of GSH with Cd and melatonin, respectively. Upon titration of GSH with Cd, an exothermic interaction with steady saturation of heat change was observed (Figure 16A). However, GSH with melatonin showed an exothermic interaction with the sequential binding pattern which was fitted to five sites sequential binding model with gradual

saturation (Figure 16B). When titration of GSH with a combination of melatonin and Cd, a significant single site binding with significant heat change was observed (area under the curve) as a progressive saturation with time (Figure 16C). As to the titration of CAT with Cd injection, a sequential binding pattern with low-intensity binding was observed and this binding was characteristic with gradual saturation of binding energy (Figure 16D). However, titration of CAT with melatonin displayed a significant one site binding with high initial heat change which slowed down with time (Figure 16E). Interestingly, upon titration of CAT with a combination of Cd and melatonin, an endothermic reaction was observed and this reaction characterized a competition between Cd and melatonin for the same binding site in CAT until the gradual saturation was reached (Figure 16F).

DISCUSSION

Involvement of oxidative stress in the initiation and

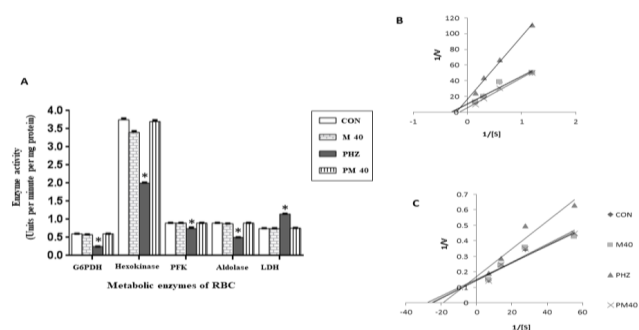


Figure 13: The Km values were calculated from LBP curves using the straight-line equation. For G6PDH, the $y = mx + c$. Vmax: Con= 0.093 mm/min, M40 = 0.1 mm/min, PHZ = 0.061 mm/min, PM40 = 0.182 mm/min; Km: Con = 3.26 mm, M40=3.57 mm/min, PHZ = 4.81 mm/min, PM40 = 6.82 mm/min. For hexokinase, $y = mx + c$. Vmax: Con = 6.9 mm/min, M40 = 6.6 mm/min, PHZ = 5.9 mm/min, PM40 = 6.9 mm/min; Km: Con = 0.035 mm, M40=0.033 mm/min, PHZ = 0.047 mm/min, PM40 = 0.035 mm/min. CON: Control; M40: Melatonin (40 nmoles/mL); PHZ: Phenylhydrazine (1 mm); PM40: Phenylhydrazine (1 mm) + Melatonin (40 nmoles/mL). The values are expressed as Means \pm SEMs ($n = 6$), *: $P \leq 0.001$ compared other groups. (Published in Paul *et al.*, Melatonin Research, 2018)²⁸

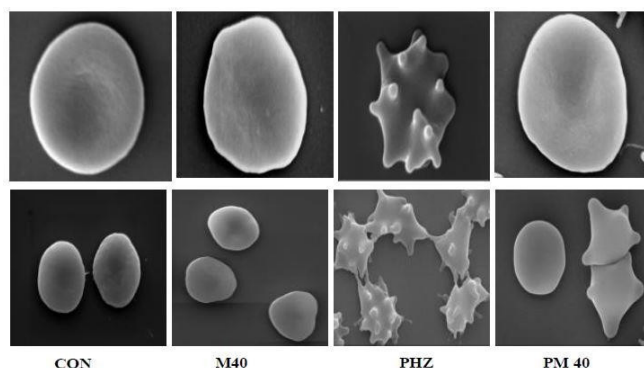


Figure 14: Upper panel (60 KX) and lower panel (35 KX). CON: Control; M40: Melatonin (40 nmoles/mL); PHZ: Phenylhydrazine (1 mm); PM40: Phenylhydrazine (1 mm) + Melatonin (40 nmoles/mL). (Published in Paul *et al.*, Melatonin Research, 2018)²⁸

progression of various diseases including ischemic heart disease has been recognized in experimental as well as in human situations.³³ Gastric endogenous melatonin has been found to be protective enough toward threats to gastric tissue system. The decrease in melatonin level in gastric system also bring a bout stress mediated harmful alterations. Our studies reveal that melatonin is capable in ameliorating the cardiac damages following ISO treatment through its antioxidant mechanisms and also by improving the cardiac functions^{2,11}. Furthermore, in the consequent studies, we attempted to further document ISO-induced myocardial damage *in vivo* and melatonin's ability to ameliorate the ISO-induced effects. Our studies clearly reveal that following ISO treatment, the activities of XO and XDH are highly significantly increased compared to control and with a concomitant increase in the XO plus XDH, XO/XDH ratio, XO/ XO + XDH ratio. This indicates that metabolic reactions involving these two enzymes serve as the source of superoxide anion free radical, ROS (Figure 1). We found a significant elevation in apaf-1 and caspase 9 protein levels because of ISO treatment (Figure 2). Apaf-1 is known to form a complex with cytochrome c, which triggers caspase 9 and, eventually, apoptosis. Interestingly, melatonin pretreatment significantly reduced the levels of both proteins indicating a protective role of this small indole against stress-induced cellular apoptosis. Melatonin's role as an antioxidant, documented earlier, is quite evident considering the reduction in superoxide anion free radical production following melatonin pretreatment. Isoproterenol-induced stress also significantly altered the levels of mitochondrial GSH, GSSG, and their ratio. The GSH-GSSG couple functions as a cellular redox buffer.³⁴ Any alteration in their concentrations results in disruption of the redox potential as was evident from our study. Co- incubation of the mitochondria with melatonin protected these changes from taking place, indicating melatonin's ability to protect the mitochondrial antioxidant status (Figure 3). The role of melatonin as a natural antioxidant may serve as a potential therapeutic agent for heart diseases that are related to oxidative stress and inflammation, particularly in those cases

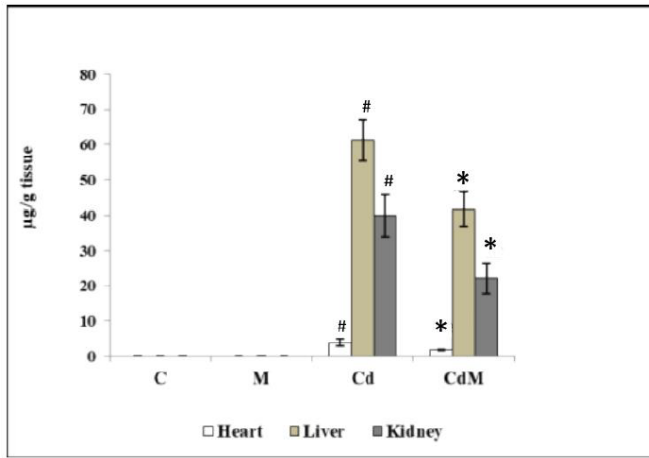


Figure 15: Effect of melatonin on the concentrations of Cd in heart, liver and kidney tissues. Data were expressed as mean ± S.E.M. (n=6). Rats were treated with CdCl₂. C: control, M: melatonin alone, Cd: cadmium alone, CdM: Cadmium plus melatonin (0.44 mg/kg) and/or, melatonin (10 mg/kg). # *p*<0.001 vs. Cd-treated group; * *p*<0.001 vs. Cd-treated group. (Published in Mitra *et al.*, Melatonin Research, 2019)²⁹

with abnormal lipid metabolism. According to the changes associated with the lipid profile of ISO-treated rats and the protection offered by melatonin pretreatment (Table 1), and also considering its low or no-toxicity, its' easy availability and inexpensiveness, melatonin should be recommended for clinical trial to evaluate its protective effects on the patients with coronary artery diseases.

As depicted herein, isoproterenol-induced increase in mitochondrial membrane potential (Figure 4) corroborated our earlier findings that ISO causes myocardial damage through disturbances in mitochondrial function. Mitochondrial Membrane Potential (MmP), measured by JC-1 staining, is an indicator for cell death or apoptosis. Decrease in MmP coincides directly with the opening of the mitochondrial membrane permeability transition pores (MPTP), resulting in the release of cytochrome c into the cytosol, which in turn leads to downstream events in the apoptotic cascade. JC-1 is a mitochondria-specific dual-fluorescent probe that exhibits a potential-dependent accumulation in mitochondria showing higher levels of accumulation in control or polarised and decreased accumulation in depolarised mitochondria that have undergone ISO treatment.

Pre- treatment of rats with melatonin at 10 mg/kg bw protected the cardiac mitochondria by scavenging ROS, decreasing MmP and thereby inhibiting the opening of the MPTP.

Isothermal titration calorimetric studies carried out in the present study *in-vitro* as well as in cell-free system with pure Cu-Zn superoxide dismutase along with different combinations of copper chloride, ascorbic acid and melatonin (Figure 5) suggests that when melatonin is present in the reaction medium along with copper-ascorbate, it restrains the copper-ascorbate molecules by binding with them physically along with scavenging the free radicals generated by them. Possibly, the binding of melatonin to these antioxidant

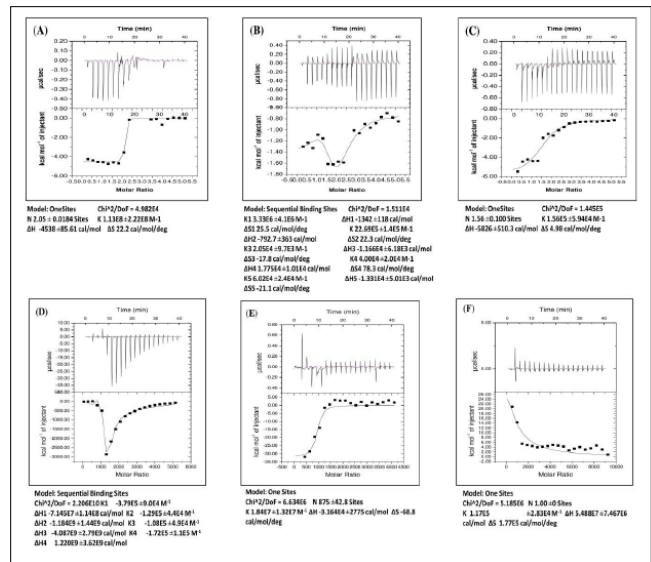


Figure 16: Binding analyses of GSH and CAT with Cd and melatonin in a cell-free/chemical system. The representative ITC profiles of GSH and CAT with Cd and melatonin. In the heat changes vs. time titration curves, each peak represents an injection of ligand into the sample cell that contains (A) GSH vsCd as ligand, (B) GSH vs melatonin as ligand, (C) GSH vs Cd and melatonin as ligands, (D) CAT vs Cd as ligand, (E) CAT vs melatonin as ligand and (F) CAT vs Cd and melatonin as ligands. The amount of heat change per second (ΔH) is represented by the area under the curve and the heat change in terms of kcal mol⁻¹ of injectant against molar ratio is shown below curve of each figure, respectively. Values of ΔH , ΔS and no. of sites were expressed in terms of mean ± S.E. (Published in Mitra *et al.*, Melatonin Research, 2019)²⁹

enzymes conceals those specific sites of these antioxidant enzymes which are susceptible to attack, thus preventing oxidative damage by copper-ascorbate molecules. To the best of our knowledge and belief, this was perhaps the first report to indicate a third mechanism, i.e., a new of action of melatonin via its receptor independent pathways.

Investigating the mechanism of ROS-mediated myocardial damage may lead to the development of new therapeutic solutions for myocardial ischemia. This study shows that melatonin ameliorates ISO-induced myocardial injury induced by ISO mediated oxidative stress and also prevents mitochondrial dysfunction in goat heart mitochondria *in-vitro*, through its antioxidant mechanisms indicating that this indole is an ideal candidate for future treatment of myocardial ischemia and other cardiovascular disorders involving mitochondrial dysfunction and generation of oxidative stress. The overall mechanism of action of melatonin toward cardiac tissue system has been presented in Figure 17.

In gastric tissue system also, melatonin has been experimented to provide enormous protection by keeping endogenous melatonin level nearly at its control level (Figure 12) and in supporting to this, preservation of morphology and architecture of different segments of gastric tissue was found to be conserved upon melatonin treatment (Figures 9, 10

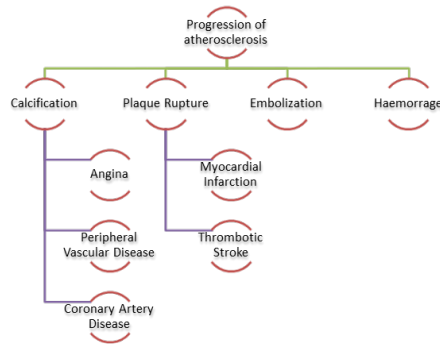


Figure 17: Schematic diagram showing protective action of melatonin toward cardiac tissue system. (Published in Datta *et al.*, Melatonin Research, 2021)³⁰

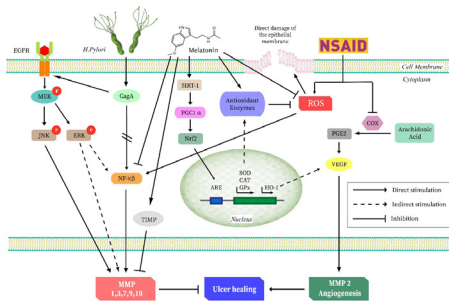


Figure 18: Schematic diagram showing protective action of melatonin toward gastric tissue system. (Published in Majumder *et al.*, Melatonin Research, 2021)³¹

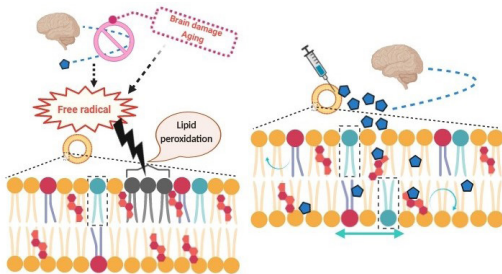


Figure 19: Schematic diagram showing membrane permeable property of melatonin for providing protection toward tissue and cellular systems. (Published in Banerjee *et al.*, Melatonin Research, 2021)³²

and 11). In specific studies, we have found that minimizing the side-effects of ranitidine and omeprazole may be possible, when their long-term use is the only choice, if co-administered with melatonin (Figure 6). Our further studies also indicated that it may be possible to minimize the gastro-toxic effects of piroxicam, when their long-term use is the only choice, if melatonin is also included in the treatment regimen. Furthermore, these studies once again establish the versatility in the action of melatonin as an antioxidant, i.e. direct scavenging actions as well as indirect antioxidant functions (Figure 7, 8).

RBC deformation was also prevented by melatonin (Figure 14). Regarding functional aspects, the metabolic enzymes were also experimented to be conserved in melatonin treated erythrocytes (Figure 13). Binding profiles of melatonin with PHZ and ferrous iron indicated favorable binding of

melatonin with both of them. Thus, in addition to the direct antioxidant and free radical scavenging capability, melatonin also inhibited iron overloading by chelating iron and binding with the PHZ. This action of melatonin further reduces free radical generation. Based on the results, melatonin may provide therapeutic relevance to β -thalassemia and other hemolytic RBC disorders involving oxidative stress.

Above all, the easy membrane permeability of melatonin for tissue and cellular system has been presented in Figure 19. The implication of its cardio-protective and gastro-protective action as well as its erythrocyte preservation acts might be mediated by this unique property of the indoleamine, which helps melatonin excel in its antioxidative as well as anti-inflammatory role.

ACKNOWLEDGEMENT

Works are partially supported by UGC Major Research Project Grant to Dr. DB [F. No. 37- 396/2009 (SR)] and also by a UPE II GRANT and a CSIR Senior Research Fellowship to Dr. Debasri Mukherjee and to Dr. Arnab Kumar Ghosh. Dr. DB also gratefully acknowledges the receipt of a major research project under Centre with Potential for Excellence in a Particular Area (CPEPA) Scheme of UGC, Govt. of India, New Delhi. Prof. DB further gratefully acknowledges the support that he received from DST PURSE Grant awarded to Calcutta University. Dr. DB also gratefully acknowledges the hard work and thoughtful research of all the research scholars who have spent some of their valuable times pursuing their research works in Dr. DB's laboratory. Dr. DB is also deeply thankful to his collaborators for their various generous help in various stages of research.

CONFLICT OF INTEREST

Nil

REFERENCES

- Reiter RJ, Tan DX. Melatonin: a novel protective agent against oxidative injury of the ischemic/reperfused heart. *Cardiovasc Res.* 2003;58(1): 10-9. PMID: 12667942.
- Mukherjee D, Roy SG, Bandyopadhyay A, Chattopadhyay A, Basu A, Mitra E, Ghosh AK, Reiter RJ and Bandyopadhyay D. Melatonin protects against isoproterenol-induced myocardial injury in the rat: antioxidative mechanisms. *J Pineal Res.* 2010;48(3):251–62. PMID: 20210856.
- Kearney J. Food consumption trends and drivers. *Philos Trans R Soc Lond, B Biol Sci.* 2010;365 (1554):2793-807. DOI: 10.1098/rstb.2010.0149.
- WHO. Diet, Nutrition and the prevention of chronic diseases. WHO Technical Report series 2003; 916,1-148. <https://apps.who.int/iris/>.
- Tsai WC, Li YH, Lin CC, Chao TH, Chen JH. Effects of oxidative stress on endothelial function after a high-fat meal. *Clin Sci.* 2004;106(3):315-9. PMID: 14561213.
- Tawfik MK, El-Kherbetawy MK & Makary S. Cardioprotective and anti- aggregatory effects of levosimendan on isoproterenol-induced myocardial injury in high-fat-fed rats involves modulation of PI3K/Akt/mTOR signaling pathway and inhibition of apoptosis: comparison to cilostazol. *J Cardiovas Pharmacol*

- Ther. 2018;23(5):456-71. PMID: 29685053.
7. Chattopadhyay A, Biswas S, Bandyopadhyay D, Sarkar C, Datta AG. Effect of isoproterenol on lipid peroxidation and antioxidant enzymes of myocardial tissue of mice and protection by quinidine. *Molecular and cellular biochemistry*, 2003; 245(1): 43- 49. PMID: 12708743.
 8. Scheibye-Knudsen M, Fang EF, Croteau DL, Wilson III DM, Bohr VA. Protecting the mitochondrial powerhouse. *Trend Cell Biol*, 2015; 25(3): 158-170. PMID: 25499735.
 9. Srinivasan V, Spence DW, Pandi-Perumal SR, Brown GM & Cardinali DP. Melatonin in mitochondrial dysfunction and related disorders. *Int J Alz Dis*. 2011;2011:326320: PMID: 21629741.
 10. Madamanchi NR, Runge MS. Mitochondrial dysfunction in atherosclerosis. *Circ Res*. 2007; 100(4): 460-473. DOI: 10.1161/01.RES.0000258450.44413.96.
 11. Mukherjee D, Ghosh AK, Bandyopadhyay A, *et al*. Melatonin protects against isoproterenol-induced alterations in cardiac mitochondrial energy-metabolizing enzymes, apoptotic proteins, and assists in complete recovery from myocardial injury in rats. *J Pineal Res*. 2012;53(2):166-79. PMID: 23050266.
 12. Naaz S, Mishra S, Pal PK, Chattopadhyay A, Das AR, Bandyopadhyay D. Activation of SIRT1/PGC 1 α /SIRT3 pathway by melatonin provides protection against mitochondrial dysfunction in isoproterenol induced myocardial injury. *Heliyon*, 2020; 6(10): e05159. PMID: 33088945.
 13. Bose G, Ghosh A, Chattopadhyay A, Pal PK, Bandyopadhyay D. Melatonin as a potential therapeutic molecule against myocardial damage caused by high fat diet (HFD). *Melatonin Res*. 2019;2(3):37-56. DOI: 10.32794/mr11250030.
 14. Ghosh A, Bose G, Dey T, *et al*. Melatonin protects against cardiac damage induced by a combination of high fat diet and isoproterenol exacerbated oxidative stress in male Wistar rats. *Melatonin Res*. 2019;2(1):9-31. DOI: 10.32794/mr11250030.
 15. Ghosh AK, Naaz S, Bhattacharjee B, *et al*. Mechanism of melatonin protection against copper- ascorbate-induced oxidative damage *in-vitro* through isothermal titration calorimetry. *Life Sci*. 2017;180:123-36. PMID: 28528861.
 16. Roy A, Ganguly A, Bose SD, Das BB, Pal C, Jaisankar P, Majumder HK. Mitochondria-dependent reactive oxygen species-mediated programmed cell death induced by 3, 3'-diindolylmethane through inhibition of F0F1-ATP synthase in unicellular protozoan parasite *Leishmaniadonovani*. *Mol Pharmacol*. 2008;74(5):1292-307. PMID: 18703668.
 17. Greenlee L, Handler P. Xanthine oxidase VI. Influence of pH on substrate specificity. *J Biol Chem*. 1964;239(4):1090-5. PMID: 14165912.
 18. Bandyopadhyay D, Ghosh G, Bandyopadhyay A, Reiter RJ. Melatonin protects against piroxicam-induced gastric ulceration. *J Pineal Res*. 2004;36(3):195-203. PMID: 15009511.
 19. Cossarizza A, Salvioli S. Flow cytometric analysis of mitochondrial membrane potential using JC-1. *Curr Prot Cytometry*. 2000;13(1):9-14. PMID: 18770751.
 20. Rajarathnam K, Rösger J. Isothermal titration calorimetry of membrane proteins— Progress and challenges. *Biochim Biophys Acta Biomem*. 2014; 1838(1): 69- 77. PMID: 23747362.
 21. Das D, Bandyopadhyay, D, Bhattacharjee, M, Banerjee RK. Hydroxyl radical is the major causative factor in stress-induced gastric ulceration. *Free Rad Biol Med*. 1997; 23(1): 8-18. DOI: 10.1016/S0891-5849(96)00547-3.
 22. Chen CQ, Fichna J, Bashashati M, Li, YY, Storr M. Distribution, function and physiological role of melatonin in the lower gut. *World J Gastroenterol*. 2011;17(34):3888–98. DOI: 10.3748/wjg.v17.i34.3888.
 23. Pajaniradje S, Mohankumar K, Pamidimukkala R, Subramanian S, Rajagopalan R. Antiproliferative and apoptotic effects of *Sesbania grandiflora* leaves in human cancer cells. *BioMed Res Int*. 2014; 2014:474953. PMID: 24949454.
 24. Cheema K. J, Scofield A. M. Scanning electron microscopy of the intestines of rats infected with *Nippostrongylus brasiliensis*. *Int J Parasitol*. 1982;12(2-3):199–205. DOI: 10.1016/0020-7519(82)90017-0.
 25. Mukherjee D, Ghosh AK, Dutta M, Mitra E, Mallick S, Saha B, Reiter RJ, Bandyopadhyay D. Mechanisms of isoproterenol-induced cardiac mitochondrial damage: protective actions of melatonin. *J Pineal Res*. 2015;58(3):275-90. PMID: 25652673.
 26. Bandyopadhyay D, Bandyopadhyay A, Das PK, Reiter RJ. Melatonin protects against gastric ulceration and increases the efficacy of ranitidine and omeprazole in reducing gastric damage. *J Pineal Res*. 2002;33(1):1-7. DOI: 10.1034/j.1600-079x.2002.01107.x.
 27. Pal PK, Sarkar S, Mishra S, Chattopadhyay S, Chattopadhyay A, Bandyopadhyay D. Amelioration of adrenaline induced oxidative gastrointestinal damages in rat by melatonin through SIRT1-NF κ B and PGC1 α -AMPK α cascades. *Melatonin Res*. 2020;3(4):482-502. DOI: 10.32794/mr11250074.
 28. Paul S, Naaz S, Ghosh AK, Mishra S, Chattopadhyay A, Bandyopadhyay D. Melatonin chelates iron and binds directly with phenylhydrazine to provide protection against phenylhydrazine induced oxidative damage in red blood cells along with its antioxidant mechanisms: an *in-vitro* study. *Melatonin Res*. 2018;1(1):1-20. DOI: 10.32794/mr11250001.
 29. Mitra E, Bhattacharjee B, Pal PK, *et al*. Melatonin protects against cadmium-induced oxidative damage in different tissues of rat: a mechanistic insight. *Melatonin Res*. 2019;2(2):1-21. DOI: 10.32794/mr11250018.
 30. Datta M, Majumder R, Chattopadhyay A, Bandyopadhyay D. Protective effect of melatonin in atherosclerotic cardiovascular disease: A comprehensive review. *Melatonin Res*. 2021;4(3): 408-30. DOI: 10.32794/mr112500102.
 31. Majumder R, Datta M, Chattopadhyay A, & Bandyopadhyay D. Melatonin promotes gastric healing by modulating the components of matrix metalloproteinase signaling pathway: a novel scenario for gastric ulcer management. *Melatonin Res*. 2021;4(2):213-31. DOI: 10.32794/mr11250092.26.
 32. Banerjee A, Chattopadhyay A, Bandyopadhyay D. Melatonin and biological membrane bilayers: a never ending amity. *Melatonin Res*. 2021; 4(2): 232-52. DOI: 10.32794/mr11250093.
 33. Chagoya de Sánchez V, Hernández-Muñoz R, López-Barrera F, Yañez L, Vidrio S, Suárez J, Cota-Garza MD, Alberto AF, Cruz D. Sequential changes of energy metabolism and mitochondrial function in myocardial infarction induced by isoproterenol in rats: a long-term and integrative study. *Canadian J Physiol Pharmacol*, 1997; 75 (12): 1300-11. PMID: 9580216.
 34. Schafer FQ, Buettner GR. Redox environment of the cell as viewed through the redox state of the glutathione disulfide/ glutathione couple. *Free Rad Biol Med*. 2011; 30 (11): 1191-212. PMID: 11368918.